ISSN 1330-3651 (Print), ISSN 1848-6339 (Online)
https://doi.org/10.17559/TV-20241128002156
Original scientific paper

Design and Evaluation of a Compact Wide-Band Antenna for Wearable Wireless Applications

A. ANAND BABU*, K. THENMALAR

Abstract: This article presents a compact wide-band antenna designed for emerging wireless applications. The antenna utilizes a fiberglass-reinforced (FR4) substrate material with a thickness of 1.6 mm as its base. By varying the length and side edge dimensions of the antenna element, the design achieves a wide operational bandwidth ranging from 3.2 to 3.8 GHz, covering all new radio bands. Experimental optimization of various parameters has been conducted to ensure precise tuning within the desired frequency range. The antenna exhibits a uniform radiation pattern across its operating band, ensuring stable performance. Specific Absorption Rate (SAR) evaluations, conducted as per the Federal Communications Commission (FCC) guidelines, confirm the SAR values remain within the prescribed safety limit of 1.6 W/kg when the antenna is positioned on a human phantom model. The proposed antenna also demonstrates high radiation efficiency and peak gain, making it suitable for wearable applications where compact size and reliable performance are critical. This innovative design addresses the growing demand for wide-band antennas in wireless communication systems, emphasizing safety, efficiency, and adaptability for wearable technologies.

Keywords: FR4 substrate; radiation efficiency; specific absorption rate (SAR); wide-band antenna; wearable applications

1 INTRODUCTION

The mobile wireless communication technology has been started with 2G with the extension of Global System for Mobile communication (GSM) and it has been extended to 3G and 4G and finally expanded its communication ranges to packet optimization systems, such as 3.5G and 4G, more than 20 years ago. More data may now be transported more quickly thanks to the recent approval of new 5G frequency channels. The modern mobile and wireless communication era uses higher end smartphones which have a single antenna element which can be operating for various wireless standard purposes such as in Internet of Things (IoT) and all higher end standards [1-4].

A thorough examination of mobile communications antennas may be found in References . Almost all of these antennas only work with two or three different frequency ranges at the same time. There have been some antennas that could work with frequencies up to 5 - 6 GHz [5-7]. The fourth generation wireless communication infrastructure has encountered numerous issues with people's constant requirements for higher utilization of the bandwidth. Low latency and large data rates are not achievable with the current wireless infrastructure. As a result, the fifth generation has now been made available, which promises to simultaneously satisfy the demands for faster data rates and a lower degree of latency.

In communication systems, antennas are very important. They are used to send and receive messages. Excellent antennas must be utilized in order to fulfill the increasingly demanding demands for new systems. There is a need for utilizing broad band antennas which can be used in multiband and high frequency devices. In order to satisfy such criteria, patch antenna has been developed. By its minimized antenna element size and cost optimization, it has paid higher attention in wireless communication standards [8-12].

There were a lot of ideas for microstrip patch antennas that could have a wide bandwidth so that they could cover the whole 5G spectrum. These antennas, on the other hand, are very complicated to make and very big. The important criteria during the utilization of antenna in wireless communication is its size while operating in wide band frequency patterns. Hence, monopole and helical antenna elements have been used which satisfied the above criteria [13, 14].

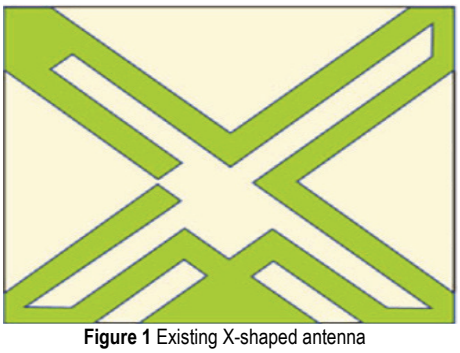


Figure 1 Existing X-shaped antenna

A patch antenna is used in biomedical implants. The High Frequency Simulation Software (HFSS) is used to design the X-shaped antenna (Fig. 1). This resonates at 915 MHz in the ISM band. The antenna's full dimensions are made of Rogers material called RT/Duroid 5880 which is very expensive when it is employable for commercial applications. Since the antennas shown in the literature are not appropriate for the new wireless technology being used, this study discusses the design of a wideband antenna element pattern which can be used for 5G wireless standards at 6 GHz. Because of its unique structural features, it has been identified as the novel design pattern for various wireless applications. In addition, the results and discussion section contains a remark and record of the obserevd parameters. Finally, a small wideband antenna has been constructed and presented in this study, with the major goal to achieve a low range of return loss which it exhibits at 3.3-3.8 GHz frequency range [15-18].

2 PROPOSED SYSTEM

The overall structure of the proposed antenna and its prototype have been depicted in Fig. 2. The 1.6 mm thick FR4 substrate has been used in this design where R_1 and R_2

have been placed in its front side portion. This radiating concentric circle is fed by the feeding line of length $L_1 \times W_1$. There are three phases involved in creating the ground plane on the substrate's rear side. Firstly, the ground plane is formed by making rectangular shape of size $L \times W_2$ mm^2. Secondly, a small rectangular slot of dimension $L_2 \times W_3$ mm^2 has been carved.

The use of FR4 substrate in the proposed antenna provides several advantages, including mechanical stability and durability, which are crucial for wearable applications where the antenna needs to withstand bending and environmental stresses. FR4 is also cost-effective and easy to fabricate, making it an attractive choice for mass production. However, it has some limitations, particularly its dielectric constant and loss tangent, which can reduce radiation efficiency, especially at higher frequencies. Additionally, FR4's limited flexibility compared to textile or polymer-based substrates may affect performance in highly dynamic, flexible environments. Alternatives like flexible polymers or textiles offer higher flexibility and potentially lower losses but may sacrifice mechanical strength or cost efficiency.

At last, two triangular shaped slots are etched along two side corners of ground region with the dimension $L_3 \times W_4$ as shown in Fig. 2b. The complete antenna is printed on the substrate of area $L \times W$ mm^2 and its fabricated frint view and back view representation have been given in Fig. 2c and Fig. 2d respectively. The detailed design parameters have been illustrated in Tab. 1.

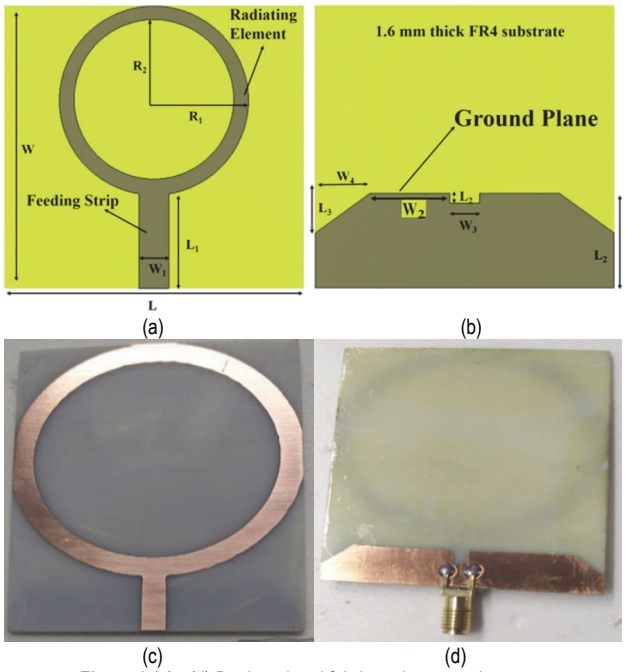


Figure 2 (a) - (d) Designed and fabricated antenna images

Table 1 Detailed dimension of the proposed broad-band antenna

R_1	R_2	L	L_1	L_2	L_3	W	W_1	W_2	W_3	W_4
19	16	28.5	9.5	1	4	30	3	9.5	3	5

Fig. 3 shows the above antenna design's simulated and measured scattering parameter values.

This antenna design exhibits the frequency spectrum of 3.2-3.8 GHz which includes all new radia bands over the 10 dB impedance bandwidth.

One of the challenges of the proposed antenna design lies in the use of the fiberglass-reinforced (FR4) substrate, which, despite being cost-effective and easily accessible, may impose limitations on performance. FR4's relatively high dielectric loss tangent could reduce radiation efficiency, especially at higher frequencies, potentially affecting the antenna's overall performance in specific applications. Furthermore, the mechanical rigidity of the FR4 substrate might limit its adaptability in scenarios requiring high flexibility, such as in wearable devices. Additionally, while the wide operational bandwidth (3.2 to 3.8 GHz) is an advantage, achieving uniform performance across such a broad range may require careful tuning of antenna parameters, making the design process more complex. Finally, the safety evaluation based on the Specific Absorption Rate (SAR) remains confined to a human phantom model, which may not entirely reflect real-world conditions, such as different body positions or environmental factors.

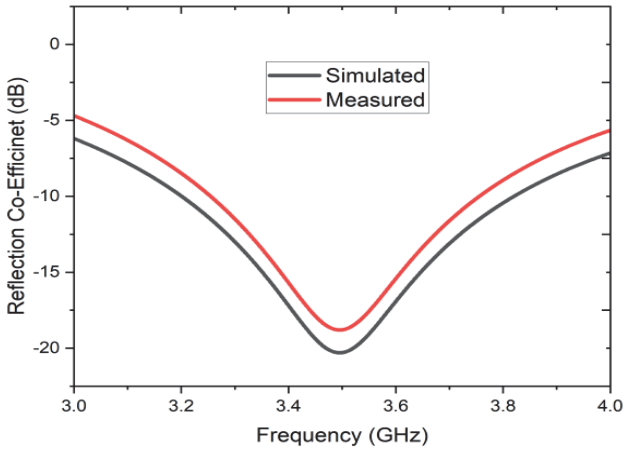


Figure 3 Reflection co-efficient

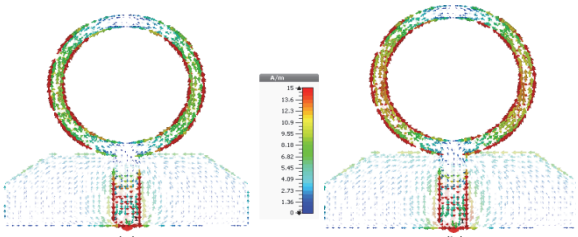
The proposed antenna outperforms several designs in the literature by offering a compact size (28.5 × 30 × 1.6 mm) and utilizing a defected ground structure (DGS) to enhance bandwidth and efficiency, making it more suitable for wearable applications. Compared to other designs like [19] (46 × 4 × 0.04 mm) and [4] (40 × 30 × 1.4 mm), the proposed antenna is smaller, yet it maintains a reasonable gain of 3 dBi, higher than some designs such as [19] (2.72 dBi) and [20] (3 dBi). While antennas like [25] exhibit higher gains (24.3 dBi), the proposed antenna's gain is practical for compact wearable devices. Additionally, its operational frequency of 2.45 GHz aligns with widely-used wireless communication systems, providing reliable performance for typical applications. The use of copper as the radiating material, combined with the DGS design, offers a good balance of performance, cost, and integration potential. Overall, the proposed antenna provides a more efficient, smaller, and adaptable solution for wearable technologies compared to other designs in the literature.

3 PARAMETRIC ANALYSIS

Initially a circle of radius 19 mm along with feed line has been kept as radiating element along with uniform ground plane. The antenna shown in iteration 1 has very poor radiation performance as listed in Tab. 1. After

removing some major part of the radiating element with uniform ground plane has been obtained due to iteration1 modifications. Still the antenna (iteration 2) does not meet the required band of resonance. Therefore, length of the ground plane has been reduced to 9.5 mm, thereby the antenna has some effects on resonance near required band of operation as shown in iteration 3. Further, in order to improve the frequency response, two triangular slots have been etched by iteration 4.

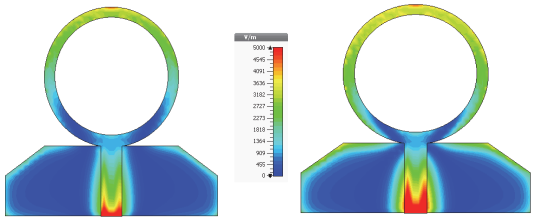
The antenna shown in iteration 4 has some good resonance in terms of reflection co-efficient with some frequency deviation from actual frequency of operation (3.2-3.8 GHz). Finally, a small rectangular slot of size 3×1.5 mm^2 has been placed out in iteration 5 with frequency band of operation 3.2-3.8 GHz over 10 dB resonance.



(a) (b)

Figure 4 The current pattern circulating the radiating element at (a) 3.45 GHz, (b) 3.7 GHz

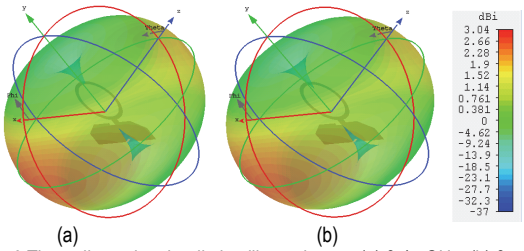
Fig. 4a and Fig. 4b illustrate the surface current distribution analysis with respect to various frequency ranges at 3.45 GHz, and at 3.7 GHz respectively. In both cases the peak current distribution is observed along edges of concentric circle. It reveals that the frequency range 3.2 GHz to 3.8 GHz exhibits only due to the impact of the concentric radiating circles.



(a) (b)

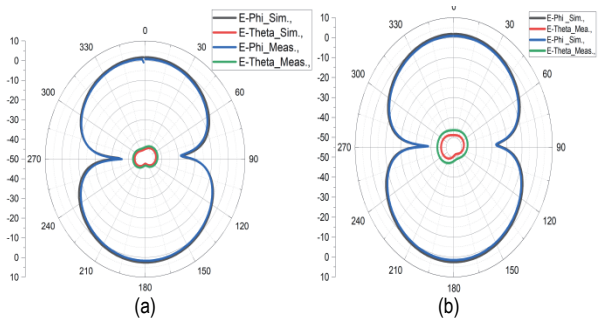
Figure 5 Electric field distribution over the radiating circle at (a) 3.45 GHz; (b) 3.7 GHz

Similarly, E-field analysis has been depicted in Fig. 5a and Fig. 5b. One can see that the maximum E-field distribution has been observed along the top edge of the radiating element which is just opposite to the location where peak current distribution is observed. It proves the proposed antenna has followed boundary conditions significantly.



(a) (b)

Figure 6 Three dimensional radiation illustrations at (a) 3.45 GHz; (b) 3.7 GHz



(a) (b)

Figure 7 a) 3.45 GHz frequency based radiation structure, (b) 3.7 GHz based radiation structure

Fig. 6a and Fig. 6b shows the 3D- graph analysis of radiation pattern at 3.45 GHz and at 3.7 GHz respectively. It is observed that, throughout the band of operation the antenna has unique radiation charecteristics with maximum gain of 3.04 dBi which is significant for a device for 5G applications and also the antenna has dipole like radiation pattern in its spacific frequency pattern.

The E-theta and E-phi result analyses have been depicted in Fig. 7a and Fig. 7b with respect to the simulation and measurement results of the design at 3.45 GHz and at 3.7 GHz. The radiation pattern with cross-polarization has been obtained as low as −40 dB and no deep null anywhere in the pattern.

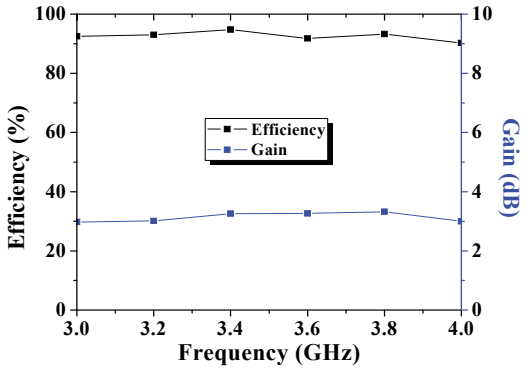


Figure 8 Graph illustrating efficiency and gain values

Throughout the operating band, the antenna's overall efficiency is between 91% and 93%, which is especially important for upcoming 5G applications. It also obtained a large gain of about 3.24 dBi. When attached to the human body, the antenna significantly affects both entire portion of the body and the bending motions of the body. As a result, it is more challenging to analyze wearable antennas than on-body antennas.

The suggested antenna is further tested in a wearable construction with an on-body layout to better understand the MIMO Antenna performance, as illustrated in Fig. 10. Since the human body moves and folds in different ways and has a lossy nature, the antenna is linked to the human body. As a result, it is difficult to evaluate antenna performance in physiological contexts. The skin, fat, muscle, and other layers that make up the human body are only a few examples. Each layer has a distinct, frequency-dependent dielectric property.

Table 2 Illustration of observed SAR values

SAR / W/Kg	3.3 GHz	3.5 GHz	3.7 GHz
1 g	0.8965	0.92356	0.9578
10 g	0.98756	0.9658	0.989745

Illustration of observed SAR values is shown in Tab. 2.

Comparative analysis with similar wide-band wearable antennas is given in Tab. 3.

Table 3 Comparative analysis with similar wide-band wearable antennas

Reference	Radiating material	Antenna dimension	Type of the antenna	Gain / dBi	Operating Frequency / GHz
[19]	Silver	46 × 4 × 0.04	CPW design	2.72	1.8
[20]	Electro-textile material	40 × 30 × 1.4	Rectangular	3	1.575
[21]	Copper	5 × 3 × 0.1	Folding antenna with double layer	1.65	2.45
[22]	Copper	10 × 10 × 1.4	Aperture-coupled	6	2.45
[23]	Copper	30 × 40 × 0.75	Circular patch	4	3.1 - 12
[24]	Copper	78 × 40 × 0.254	Serpentine structures	2.2	2.45
[25]	Copper	95.4 × 46 × 2.9	Leaky wave antenna	24.3	60
Proposed antenna	Copper	28.5 × 30 × 1.6	Defected Ground Structure	3	2.45

The proposed antenna outperforms several designs in the literature by offering a compact size (28.5 × 30 × 1.6 mm) and utilizing a defected ground structure (DGS) to enhance bandwidth and efficiency, making it more suitable for wearable applications. Compared to other designs like [19] (46 × 4 × 0.04 mm) and [4] (40 × 30 × 1.4 mm), the proposed antenna is smaller, yet it maintains a reasonable gain of 3 dBi, higher than some designs such as [19] (2.72 dBi) and [20] (3 dBi). While antennas like [25] exhibit higher gains (24.3 dBi), the proposed antenna's gain is practical for compact wearable devices. Additionally, its operational frequency of 2.45 GHz aligns with widely-used wireless communication systems, providing reliable performance for typical applications. The use of copper as the radiating material, combined with the DGS design, offers a good balance of performance, cost, and integration potential. Overall, the proposed antenna provides a more efficient, smaller, and adaptable solution for wearable technologies compared to other designs in the literature.

On and off bodys parameter graph analysis has been depicted in Fig. 10. This proposed antenna may nevertheless function dependably within the required frequency range, which has been described in this article, and is a good fit for wearable applications.

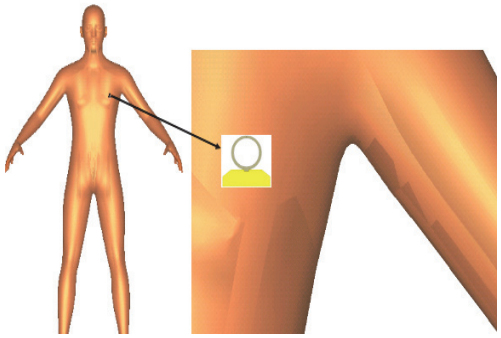


Figure 9 On-phantom position on human body

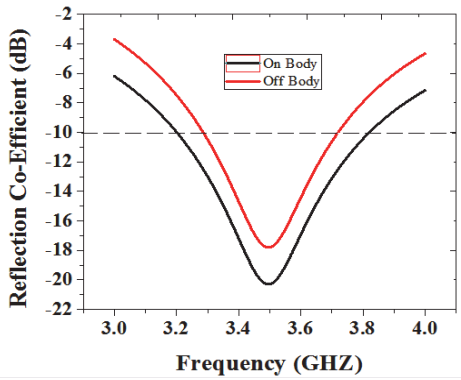


Figure 10 Performance based on ON and OFF body as wearable device

The SAR parameter has been observed after placing designed antenna on human body phantom model as shown in Fig. 11. It is found that maximum SAR obtained up to 1.6 W/Kg which is allowable limit by FCC. A thorough evaluation of the suggested antenna's performance comparison has been conducted and is shown in Tab. 2. It appears that the suggested antenna performs significantly better than the other antennas described in the literature. The proposed antenna is 3 times smaller overall than other antennas, as seen by the comparison. The antenna can function effectively in terms of other criteria despite its reduced size. The characteristics of the antenna have shown exceptional performance in both the radiation and SAR evaluations.

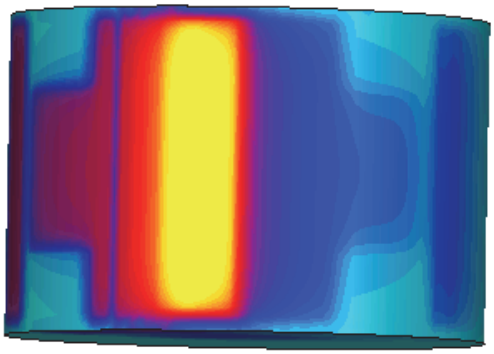


Figure 11 SAR of the proposed antenna

The SAR parameter has been observed after placing designed antenna on human body phantom model as shown in Fig. 12. It is found that maximum SAR obtained up to 1.6 W/Kg which is allowable limit by FCC. A thorough evaluation of the suggested antenna's performance comparison has been conducted and is shown in Tab. 4. It appears that the suggested antenna performs significantly better than the other antennas described in the literature. The proposed antenna is 3 times smaller overall than other antennas, as seen by the comparison. The antenna can function effectively in terms of other criteria despite its reduced size. The characteristics of the antenna have shown exceptional performance in both the radiation and SAR evaluations.

The SAR evaluation process involves assessing the electromagnetic energy absorption rate by the human body when exposed to the antenna's radiated field. This is typically performed using simulation tools like CST or HFSS, incorporating a human phantom model that mimics the dielectric properties of biological tissues, such as permittivity and conductivity. The antenna is positioned close to the phantom in scenarios replicating its intended

wearable application, such as on the chest or wrist. The input power, often standardized to 1 W, is used to evaluate SAR levels at specific distances. SAR values are calculated over a 1 gram or 10 gram volume of tissue, as per regulatory guidelines (e.g., FCC). Compliance is achieved if the SAR remains below 1.6 W/kg for 1 gram of tissue or 2 W/kg for 10 grams, ensuring the design is safe for wearable use.

The described wide-band antenna has significant potential in a variety of wearable applications beyond standard wireless communication. It can support health monitoring devices by enabling continuous data transmission in medical wearables, such as ECG monitors or blood pressure sensors, operating within new radio bands. For fitness trackers, the antenna ensures reliable connectivity for real-time data synchronization with smartphones or cloud systems. In industrial safety applications, it could enhance the performance of wearable sensors used for monitoring worker health and environmental conditions in hazardous areas. Smart textiles, including clothing embedded with sensors for athlete performance tracking or military applications, could also benefit from the antenna's compact size and efficiency.

Regarding environmental performance, the antenna's operation in wearable settings demands robust performance under diverse conditions, including body proximity effects, bending, and exposure to varying temperatures and humidity. The use of FR4 substrate offers mechanical stability, but further testing under environmental stresses like sweat, rain, and dust exposure is crucial to evaluate its reliability. Additionally, its radiation pattern stability near the human body must be maintained to prevent performance degradation due to detuning or increased SAR. Incorporating waterproofing or hydrophobic coatings could enhance durability in outdoor or high-moisture scenarios, making the design more versatile for demanding environments.

The mechanical durability of the proposed antenna in wearable conditions may be limited by the rigid FR4 substrate, which could crack or degrade under frequent bending and stretching. To improve durability and integration, alternative flexible substrates like polyamide (PI) or liquid crystal polymer (LCP) could be used, offering greater flexibility and resistance to deformation. Additionally, miniaturization techniques, such as fractal designs or microstrip patches, can reduce the antenna's size while maintaining performance. Advanced fabrication methods like inkjet printing or 3D printing, along with meta-materials or nanomaterials, can further enhance compactness, flexibility, and mechanical robustness, making the antenna more suitable for wearable applications.

In wearable environments, the proposed antenna design may face several limitations and challenges. The use of an FR4 substrate, while beneficial for its cost and ease of fabrication, presents challenges in terms of flexibility and comfort. FR4's rigid nature could cause discomfort when the antenna is worn for extended periods, particularly if the wearable device needs to conform to various body shapes or is subjected to bending or stretching. Additionally, FR4's relatively high dielectric loss may degrade performance in wearable applications, where factors like body proximity and motion could alter the antenna's efficiency and signal quality. The wide operational bandwidth (3.2 to 3.8 GHz) may also be challenging to maintain in a dynamic wearable environment, where physical obstructions or changes in orientation can lead to shifts in antenna performance. Although the SAR evaluations meet safety standards under controlled conditions, real-world wearable scenarios-where the antenna may be subjected to varying body positions, motions, and environmental factors-could cause fluctuating SAR values, requiring further optimization for safety assurance. Lastly, while the antenna demonstrates high radiation efficiency and peak gain, ensuring consistent performance in dynamic conditions, such as movement or interaction with other electronic devices, could be a challenge for maintaining stable wireless connectivity in wearable applications.

4 CONCLUSIONS

This A compact Defected Ground Structure based broad-band antenna for 5G applications has been successfully explored with outstanding radiation characteristics. The proposed antenna has covered all the frequency bands available for 5G communication under the sub 6 GHz spectrum. The antenna covered the spectrum from 3.2-3.8 GHz with 2:1 Voltage Standing Wave Ratio (VSWR). With a realized gain of 3.2 dBi, overall radiation efficiency is reached up to 92% across the spectrum. Additionally, the antenna's consistent radiation pattern within the intended operating band makes it distinct from other antennas of its kind. The design insights of the antenna have been clearly examined and tuned properly to have a substantial performance. Therefore, the antenna proposed here is one of the better designs for future bio-medical communication. After placing the designed antenna at various locations on the phantom, its performance was also investigated based on phantom design. It demonstrates that an antenna operates with almost the same efficiency whether a human is actually there or not. Finally it has been concluded that the suggested antenna may wind up being the top choice for upcoming Internet of Things applications.

5 REFERENCES

[1] Jansirani, G. & Raj, R. G. (2024). Miniaturized wide and dual-band reconfigurable antenna on-demand for portable wireless devices. *Tehnički vjesnik*, *31*. https://doi.org/10.17559/TV-20240122001282

[2] Liu, K., Chen, X., Wang, X., Zhang, Y., & Lin, S. (2021). Design of conformal spiral dual-band antenna for wireless capsule system. *IEEE Access*, *9*, 117349-117357. https://doi.org/10.1109/ACCESS.2021.3106735

[3] Banu, M. F. & Devi, B. A. (2024). A novel microwave imaging approach using rectangular antenna with complementary split-ring resonator. *Technical Gazette*, *31*(5), 1696-1703. https://doi.org/10.17559/TV-20231231001240

[4] Khan, J., Sehrai, D. A., Khan, M. A., Khan, H. A., Ahmad, S., Ahmad, S., Ali, A., Arif, A., Memon, A. A., & Khan, S. (2019). Design and performance comparison of rotated Y-shaped antenna using different metamaterial surfaces for 5G mobile devices. *Computational Materials Continua*, *2*, 409-420. https://doi.org/10.32604/cmc.2019.07001

[5] Sharaf, M. H., Zaki, A. I., Hamad, R. K., & Omar, M. M. M. (2020). A novel dual-band (38/60 GHz) patch antenna for 5G mobile handsets. *Sensors*, *20*(2541). https://doi.org/10.3390/s20092541

[6] Barreto, A. N., Faria, B., Almeida, E., Rodriguez, I., Lauridsen, M., Amorim, R., & Vieira, R. (2016). 5G-Wireless communications for 2020. *Journal of Communication and Information Systems*, *31*, 146-163. https://doi.org/10.14209/jcis.2016.22

[7] Guo, J. L., Zou, Y. L., & Liu, C. (2011). Compact broadband crescent moon-shape patch-pair antenna. *IEEE Antennas and Wireless Propagation Letters*, *10*, 435-437. https://doi.org/10.1109/LAWP.2011.2135870

[8] Chung, K. L. & Chaimool, S. (2011). Triple-band CPW-fed L-shaped monopole antenna with small ground plane. *Microwave and Optical Technology Letters*, *53*(10), 2274-2277. https://doi.org/10.1002/mop.26239

[9] Chaimool, S. & Chung, K. L. (2009). CPW-fed mirrored-L monopole antenna with distinct triple bands for WiFi and WiMAX applications. *Electronics Letters*, *45*(18), 928-929. https://doi.org/10.1049/el.2009.1439

[10] Chung, K. L., Xie, S., Li, Y., Liu, R., Ji, S., & Zhang, C. (2018). A circular polarization reconfigurable Meng-shaped patch antenna. *IEEE Access*, *6*, 51419-51428. https://doi.org/10.1109/ACCESS.2018.2869410

[11] Kamaruddin, R. A. A., Ibrahim, I. B. M., Al-Gburi, A. J. A., Zakaria, Z., Shairi, N. A., Rahman, T. A., & Purnamirza, T. (2021). Return loss improvement of radial line slot array antennas on closed ring resonator structure at 28 GHz. *Przegląd Elektrotechniczny*, *1*(5), 67-71. https://doi.org/10.15199/48.2021.05.15

[12] Al-Gburi, A. J. A., Ibrahim, I. M., & Zakaria, Z. (2017). Band-notch effect of U-shaped split ring resonator structure at ultra-wideband monopole antenna. *International Journal of Applied Engineering Research*, *12*(15), 4782-4789.

[13] Keriee, H. H., Rahim, M. K. A., Nayyef, N. A., Zakaria, Z., & Al-Gburi, A. J. A. (2020). High gain antenna at 915 MHz for off-grid wireless networks. *Bulletin of Electrical Engineering and Informatics*, *9*(6), 2449-2454. https://doi.org/10.11591/eei.v9i6.2192

[14] Abdulhameed, M. K., Kod, M. S., & Al-Gburi, A. J. A. (2021). Enhancement of elevation angle for an array leaky-wave antenna. *Przegląd Elektrotechniczny*, *8*, 109-113. https://doi.org/10.15199/48.2021.08.19

[15] Al-Gburi, A. J. A., Ibrahim, I. M., Ahmad, K. S., Zakaria, Z., Zeain, M. Y., Abdulhameed, M. K., & Saeidi, T. (2021). A miniaturised UWB FSS with stop-band characteristics for EM shielding applications. *Przegląd Elektrotechniczny*, *8*, 142-145. https://doi.org/10.15199/48.2021.08.28

[16] Zeain, M. Y., Zakaria, Z., Abu, M., Al-Gburi, A. J. A., Alsariera, H., Toding, A., Alani, S., Al-Tarifi, M. A., & Al-Heety, O. S. (2020). Design of a wideband strip helical antenna for 5G applications. *Bulletin of Electrical Engineering and Informatics*, *9*(5), 1958-1963. https://doi.org/10.11591/eei.v9i5.2264

[17] Zeain, M. Y., Zakaria, Z., Abu, M., Al-Gburi, A. J. A., Alsariera, H., Toding, A., Alani, S., Al-Tarifi, M. A., Al-Heety, O. S., Lago, H., & Saeidi, T. (2020). Design of helical antenna for next-generation wireless communication. *Przegląd Elektrotechniczny*, *11*, 96-99. https://doi.org/10.15199/48.2020.11.25

[18] Roja, G., Maheswara Venkatesh, P., & Jayasankar, T. (2023) Split Ring Resonator Inspired Dual-Band Monopole Antenna for ISM, WLAN, WIFI, and WiMAX Application. *Technical Gazette*, *30*(5), 1533-1538. https://doi.org/10.17559/TV-20230210000344

Contact information:

A. ANAND BABU, Assistant Professor
(Corresponding author)
Department of ECE,
Vivekanandha College of Technology,
Tiruchengode, Tamil Nadu, India
E-mail: anandbabua144@hotmail.com

K. THENMALAR, PhD, Professor
Department of EEE,
Vivekanandha College of Engineering for Women (Autonomous),
Tiruchengode, Tamil Nadu, India
E-mail: thenmalark@gmail.com